Free vibration and sound radiation of the rectangular plates based on edge-based smoothed finite element method and application of elemental radiators

†X.Y. You[1], *W. Li[1,2,3], Y.B. Chai[1], and Q.F. Zhang[1]

[1]Department of Naval Architecture and Ocean Engineering, Huazhong University of Science and Technology, China.

[2]Hubei Key Laboratory of Naval Architecture & Ocean Engineering Hydrodynamics, Wuhan City, China

[3]Collaborative Innovation Center for Advanced Ship and Deep-sea Exploration (CISSE), Shanghai, China

*Presenting author: hhxyyxy@163.com

†Corresponding author: hustliw@hust.edu.cn

Abstract

In this paper, the edge-based smoothed finite element (ES-FEM) method and application of elemental radiators is presented to solve the free vibration and sound radiation problems for the rectangular plates. The edge-based smoothed finite element is utilized for the modeling of plate structure. Three-node triangular elements is used to discretize the three-dimensional (3D) shell, due to its convenience for generating and good adaptability for complicated geometries. The system stiffness is obtained by using the strain smoothing technique over the smoothing domains, such as edge-based domain. Consequently, the employing of the strain smoothing technique can provide a proper softening effect to the FEM model, and cure the "overly-stiff" property existing in the standard FEM. Hence, this implementation can significantly improve the accuracy of the solution for free vibration. The application of elemental radiators can rapidly compute the sound radiation of the rectangular plates without fluid elements.

Keywords: the rectangular plates, free vibration and sound radiation, ES-FEM, elemental radiators.

1. Introduction

Nowadays, the plates have been used widely in many branches of structural engineering, such as aircraft, ships, bridges, buildings, etc. The vibration and sound radiation of plates have attracted engineering's more attention, due to the bad influence to structure's strength and acoustic performance.

Many researchers have carried out the analysis of plates. M. Levinson[1] studied linear elastic theoretical solution to free vibration of the simply-supported plate. Raske, Schlack and Fryba[2][3] researched dynamic response of isotropic rectangular plate under various moving loads. Gbadeyan and Oni[4] also computed dynamic response of rectangular plate under various moving loads based on the improved integral transformation method. The radiation resistance and efficiency of the plate in frequency domain was computed by using the approximate method, which has been widely applied in many research[5][6]. Williams and Maynard[7] used Rayleigh integral and Fast Fourier Transformation to solve the sound radiation of a plate.

Owing to limitations of the analytical methods, the finite element method (FEM) becomes one of the most popular numerical method to analyze plate structures. In the practical applications, lower-order Reissner-Mindlin shell elements are preferred due to its simplicity and efficiency. However, these low-order shell elements have a defect of the shear locking phenomenon, which has the root of incorrect transverse forces under bending. In order to eliminate shear locking, the discrete shear gap (DSG)[8] was used.

In order to overcome the "overly-stiff" problem in FEM, Liu[9] firstly proposed that the combination of the strain smoothing technique[10] and FEM, so-called the Smoothed Finite Element (S-FEM). In S-FEM models, the finite element mesh is used similarly as in the FEM models, however, the weak form is evaluated based on smoothing domains created from the entities of the element mesh such as cells (CS-FEM), or nodes (NS-FEM), or edges (ES-FEM)[11]. These smoothing domains are linear independent and hence ensure stability and convergence of the S-FEM models.

Due to the easy and automatic generation for complicated domains, the three-node triangular element. In this work, the discrete shear gap technique (DSG) is combined the ES-FEM to give a so-called ES-DSG element for plate analysis. The ES-DSG has a superior property compared to standard FEM. The employing of the strain smoothing technique can provide a proper softening effect to the FEM model, and cure the "overly-stiff" property existing in the standard FEM.

2. Three-node Reissner-Mindlin shell element

The middle surface of plate is defined as the reference plane, and let u, v, w be the displacements of the middle surface in the x, y, z direction, let $\beta_x, \beta_y, \beta_z$ be the rotation in the y, x, z direction, which is shown in Fig. 1.

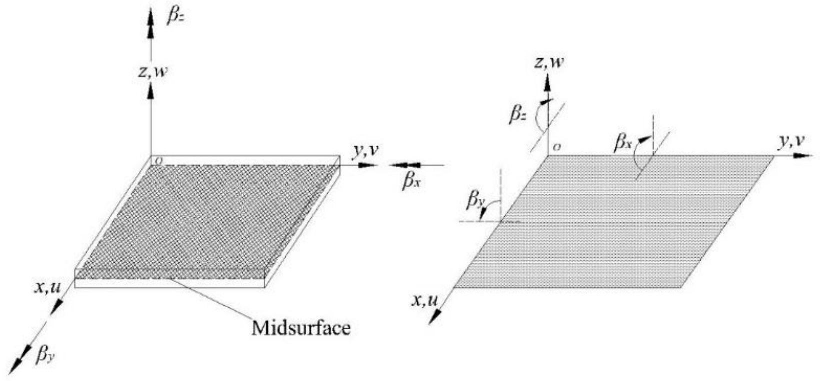

Figure 1. Reissner–Mindlin flat plate

The six independent freedom of three-node shell element at any node can be written as below, as is shown in Fig. 2.

$$\mathbf{u} = [u \ \ v \ \ w \ \ \beta_x \ \ \beta_y \ \ \beta_z]^{\mathrm{T}} \tag{1}$$

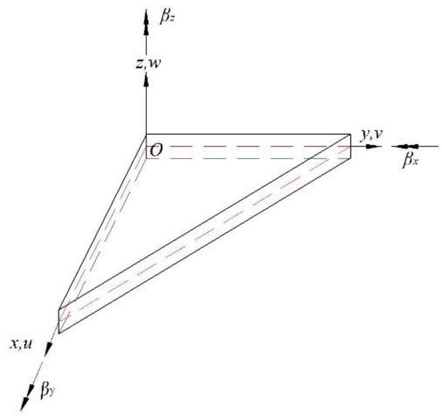

Figure 2. The three-node Reissner–Mindlin shell element

Therefore, the membrane strain ε^{m}, the curvature of the shell element κ and the shear strain γ are constructed as

$$(\boldsymbol{\varepsilon}^m)^{\mathrm{T}} = \left[\frac{\partial u}{\partial x} \ \ \frac{\partial v}{\partial x} \ \ \frac{\partial u}{\partial y} + \frac{\partial v}{\partial x} \right], \ \boldsymbol{\kappa}^{\mathrm{T}} = \left[\frac{\partial \beta_x}{\partial x} \ \ \frac{\partial \beta_y}{\partial x} \ \ \frac{\partial \beta_x}{\partial y} + \frac{\partial \beta_y}{\partial x} \right], \ \boldsymbol{\gamma} = \begin{bmatrix} \dfrac{\partial w}{\partial x} + \beta_x \\ \dfrac{\partial w}{\partial y} + \beta_y \end{bmatrix}. \tag{2}$$

For the free vibration analysis of Reissner–Mindlin shell, the standard Galerkin weak form can be written as

$$\int_{\Omega}(\delta\boldsymbol{\varepsilon}^{m})^{\mathrm{T}}\mathbf{D}^{m}\boldsymbol{\varepsilon}^{m}\ \mathrm{d}\Omega+\int_{\Omega}\delta\boldsymbol{\kappa}^{\mathrm{T}}\mathbf{D}^{b}\boldsymbol{\kappa}\ \mathrm{d}\Omega+\int_{\Omega}\delta\boldsymbol{\gamma}^{\mathrm{T}}\mathbf{D}^{s}\boldsymbol{\gamma}\ \mathrm{d}\Omega+\int_{\Omega}\delta\mathbf{u}^{\mathrm{T}}\mathbf{m}\ddot{\mathbf{u}}\ \mathrm{d}\Omega=0 \quad \textbf{(3)}$$

where $\mathbf{m}$ is the mass matrix containing the density of the material ρ and thickness of the plate t as

$$\mathbf{m}=\mathrm{diag}\left[\rho t,\ \rho t,\ \rho t,\ \rho t^{3}/12,\ 0\right], \quad \textbf{(4)}$$

$$\mathbf{D}^{m}=\frac{Et}{1-v^{2}}\begin{bmatrix}1 & v & 0\\ v & 1 & 0\\ 0 & 0 & \frac{1-v}{2}\end{bmatrix}, \quad \textbf{(5)}$$

$$\mathbf{D}^{b}=\frac{Et^{3}}{12(1-v^{2})}\begin{bmatrix}1 & v & 0\\ v & 1 & 0\\ 0 & 0 & \frac{1-v}{2}\end{bmatrix}, \quad \textbf{(6)}$$

$$\mathbf{D}^{s}=\frac{Etk}{2(1+v)}\begin{bmatrix}1 & 0\\ 0 & 1\end{bmatrix}. \quad \textbf{(7)}$$

Discretize the problem domain Ω into N_e finite elements, and $\Omega=\bigcup_{e=1}^{Ne}\Omega_e$ and $\Omega_i\bigcap\Omega_j=\varnothing$ $(i\neq j)$. Consequently, the finite element displacement solution $\mathbf{u}^{\mathrm{h}}=\left[u\ \ \mathrm{v}\ \ \mathrm{w}\ \ \beta_x\ \ \beta_y\ \ \beta_z\right]^{\mathrm{T}}$ of the Reissner–Mindlin shell model is defined as

$$\mathbf{u}^{\mathrm{h}}=\sum_{I=1}^{N_n}N_I(\mathbf{x})\mathbf{I}_6\mathbf{d}_I=\sum_{I=1}^{N_n}\mathbf{N}_I\mathbf{d}_I \quad \textbf{(8)}$$

where $\mathbf{I}_6$ is the 6th rank unit matrix; N_n is the total number of nodes in the problem domain; $N_I(\mathbf{x})$ is the shape function at Ith node; $\mathbf{d}_I=\left[u_I\ \ v_I\ \ w_I\ \ \beta_{xI}\ \ \beta_{yI}\ \ \beta_{zI}\right]^{\mathrm{T}}$ is the displacement vector of Ith node.

In order to eliminate the shear locking, the “Discrete Shear Gap” method is adopted. In each triangular element, the shear strain can be written as

$$\gamma_{yz} = \sum_{I=1}^{3} \frac{\partial N_i(\mathbf{x})}{\partial y} \Delta w_{xi} + \sum_{I=1}^{3} \frac{\partial N_i(\mathbf{x})}{\partial y} \Delta w_{yi} \quad \textbf{(9)}$$

$$\gamma_{xz} = \sum_{I=1}^{3} \frac{\partial N_i(\mathbf{x})}{\partial x} \Delta w_{xi} + \sum_{I=1}^{3} \frac{\partial N_i(\mathbf{x})}{\partial x} \Delta w_{yi} \quad \textbf{(10)}$$

where Δw_{xi} and Δw_{yi} are Discrete Shear Gap at *I*th node given by

$$\begin{aligned} &\Delta w_{x1} = \Delta w_{x3} = \Delta w_{y1} = \Delta w_{y2} = 0, \\ &\Delta w_{x2} = (w_2 - w_1) + \frac{1}{2} a(\beta_{x1} + \beta_{x2}) + \frac{1}{2} b(\beta_{y1} + \beta_{y2}), \\ &\Delta w_{y3} = (w_3 - w_1) + \frac{1}{2} c(\beta_{x1} + \beta_{x3}) + \frac{1}{2} d(\beta_{y1} + \beta_{y3}). \end{aligned} \quad \textbf{(11)}$$

The a, b, c, d in Eq.11 are defined as

$$\begin{aligned} &a = x_2 - x_1, \;\; b = y_2 - y_1, \\ &c = x_3 - x_1, \;\; d = y_3 - y_1. \end{aligned} \quad \textbf{(12)}$$

where x_i and y_i (i=1-3) are the coordinates of the nodes in a triangular element.

Therefore, the membrane, bending and shear strains can be expressed in the matrix forms as

$$\boldsymbol{\varepsilon}^{\mathrm{m}} = \sum_{I} \mathbf{R}_I \mathbf{d}_I, \;\; \boldsymbol{\kappa} = \sum_{I} \mathbf{B}_I \mathbf{d}_I, \;\; \boldsymbol{\gamma}^{\mathrm{s}} = \sum_{I} \mathbf{S}_I \mathbf{d}_I \quad \textbf{(13)}$$

where

$$\mathbf{R}_I = \begin{bmatrix} N_{I,x} & 0 & 0 & 0 & 0 & 0 \\ 0 & N_{I,y} & 0 & 0 & 0 & 0 \\ N_{I,y} & N_{I,x} & 0 & 0 & 0 & 0 \end{bmatrix} \quad \textbf{(14)}$$

$$\mathbf{B}_I = \begin{bmatrix} 0 & 0 & N_{I,x} & 0 & 0 & 0 \\ 0 & 0 & 0 & N_{I,y} & 0 & 0 \\ 0 & 0 & N_{I,y} & N_{I,x} & 0 & 0 \end{bmatrix} \quad \textbf{(15)}$$

$$\mathbf{R}_I = \frac{1}{2A_e} \begin{bmatrix} A_e & 0 & b-d & \frac{ad}{2} & \frac{bd}{2} & d & \frac{-bc}{2} & \frac{-bd}{2} & -b \\ 0 & A_e & c-a & \frac{-ac}{2} & \frac{-bc}{2} & -c & \frac{ac}{2} & \frac{ad}{2} & a \end{bmatrix} \quad \textbf{(16)}$$

Thus, the global stiffness matrix $\mathbf{K}$ can be expressed as

$$\mathbf{K}=\int_{\Omega}\mathbf{R}^{\mathrm{T}}\mathbf{D}^{m}\mathbf{R}\ \mathrm{d}\Omega+\int_{\Omega}\mathbf{B}^{\mathrm{T}}\mathbf{D}^{b}\mathbf{B}\ \mathrm{d}\Omega+\int_{\Omega}\mathbf{S}^{\mathrm{T}}\mathbf{D}^{s}\mathbf{S}\ \mathrm{d}\Omega \tag{17}$$

and the global mass matrix $\mathbf{M}$ can be expressed as

$$\mathbf{M}=\int_{\Omega}\mathbf{N}^{\mathrm{T}}\mathbf{m}\mathbf{N}\ \mathrm{d}\Omega \tag{18}$$

and the load vector $\mathbf{F}$ can be defined as

$$\mathbf{F}=\int_{\Omega}p\mathbf{N}\ \mathrm{d}\Omega+\mathbf{f}^{\mathrm{b}} \tag{19}$$

For free vibration analysis of the Reissner–Mindlin shell model, we get

$$(\mathbf{K}-\omega^{2}\mathbf{M})\mathbf{d}=0 \tag{20}$$

where ω is the natural frequencies and $\mathbf{d}$ is the mode shape vectors.

3. Edge-based smoothed finite element method

The edge-based strain smoothing technique for shell elements will be implemented in the sub-domain based on edge of triangular elements. The domain is firstly discretized as triangular elements as the standard FEM. However, the numerical integrations in Eq. (17) are no longer based on triangular elements, but based on the smoothing domain Ω_k $\left(k=1,\ 2,\ \ldots,N\right)$, in which N is the total number of the edge in the problem domain. The smoothing domain of each edge k is constructed by connecting two end-points of the edge and the middle point of its surrounding triangular elements, as is shown in Fig. 3.

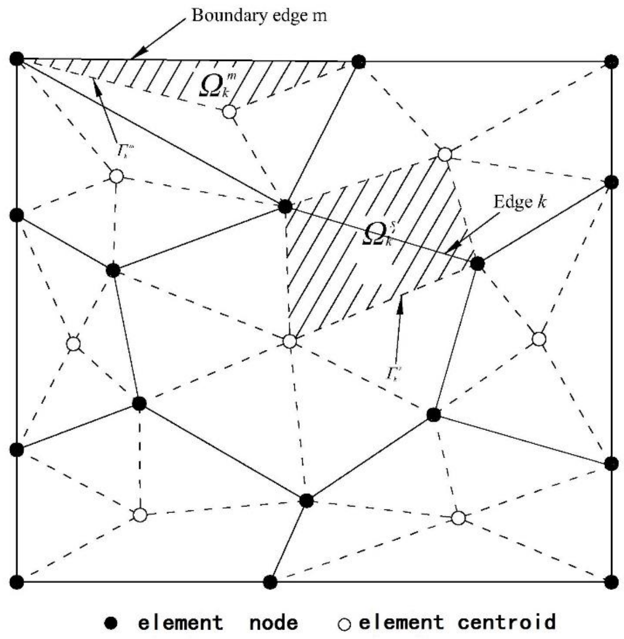

Figure 3. The edge-based smoothing domain

By using the edge-based strain smoothing technique, the integration over the whole triangular elements can be transform to an integral over the whole smoothing domains. Then, the smoothed global stiffness matrix can be rewritten as

$$\bar{\mathbf{K}}=\sum_{k=1}^{N}\left(\int_{\Omega_k}\bar{\mathbf{R}}^{\mathrm{T}}\mathbf{D}^{m}\bar{\mathbf{R}}\ \mathrm{d}\Omega+\int_{\Omega_k}\bar{\mathbf{B}}^{\mathrm{T}}\mathbf{D}^{b}\bar{\mathbf{B}}\ \mathrm{d}\Omega+\int_{\Omega_k}\bar{\mathbf{S}}^{\mathrm{T}}\mathbf{D}^{s}\bar{\mathbf{S}}\ \mathrm{d}\Omega\right) \quad \textbf{(21)}$$

Employing the strain smoothing operation over each smoothing domain on the membrane, bending and shear strains of the shell elements, the smoothing membrane, bending and shear strains over the domain Ω_k can be written as

$$\bar{\boldsymbol{\varepsilon}}^{\mathrm{m}}(\mathbf{x}_k)=\frac{1}{\mathrm{A}_k}\int_{\Omega_k}\boldsymbol{\varepsilon}^{\mathrm{m}}(\mathbf{x}_k)\ \mathrm{d}\Omega=\frac{1}{\mathrm{A}_k}\int_{\Omega_k}\mathbf{R}_k\mathbf{d}_k\ \mathrm{d}\Omega=\frac{1}{\mathrm{A}_k}\int_{\Gamma_k}\mathbf{R}_k\mathbf{d}_k\ \mathrm{d}\Gamma \quad \textbf{(22)}$$

$$\bar{\boldsymbol{\kappa}}(\mathbf{x}_k)=\frac{1}{\mathrm{A}_k}\int_{\Omega_k}\boldsymbol{\kappa}(\mathbf{x}_k)\ \mathrm{d}\Omega=\frac{1}{\mathrm{A}_k}\int_{\Omega_k}\mathbf{B}_k\mathbf{d}_k\ \mathrm{d}\Omega=\frac{1}{\mathrm{A}_k}\int_{\Gamma_k}\mathbf{B}_k\mathbf{d}_k\ \mathrm{d}\Gamma \quad \textbf{(23)}$$

$$\bar{\boldsymbol{\gamma}}^{\mathrm{s}}(\mathbf{x}_k)=\frac{1}{\mathrm{A}_k}\int_{\Omega_k}\boldsymbol{\gamma}(\mathbf{x}_k)\ \mathrm{d}\Omega=\frac{1}{\mathrm{A}_k}\int_{\Omega_k}\mathbf{S}_k\mathbf{d}_k\ \mathrm{d}\Omega=\frac{1}{\mathrm{A}_k}\int_{\Gamma_k}\mathbf{S}_k\mathbf{d}_k\ \mathrm{d}\Gamma \quad \textbf{(24)}$$

where A_k is the area of the smoothing domain Ω_k, and Γ_k is the boundary of the smoothing domain Ω_k.

After performing the integral, the smoothed membrane, bending and shear strains in the smoothing domain Ω_k can then be written in following matrix

$$\bar{\boldsymbol{\varepsilon}}^{\mathrm{m}}(\mathbf{x}_k) = \sum_{i=M_k} \bar{\mathbf{R}}_i(\mathbf{x}_k)\mathbf{d}_i \tag{25}$$

$$\bar{\boldsymbol{\kappa}}(\mathbf{x}_k) = \sum_{i=M_k} \bar{\mathbf{B}}_i(\mathbf{x}_k)\mathbf{d}_i \tag{26}$$

$$\bar{\boldsymbol{\gamma}}^{\mathrm{s}}(\mathbf{x}_k) = \sum_{i=M_k} \bar{\mathbf{S}}_i(\mathbf{x}_k)\mathbf{d}_i \tag{27}$$

where M_k is the total number of the nodes in the smoothing domain Ω_k.

4. The sound radiation analysis of plate

By employing the Rayleigh surface integral, each triangular element on the plate can be treated as a simple point source (elemental radiator) that radiating sound. Therefore, the sound pressure[12] at an arbitrary observation location Q of the plate is written as below, as is shown Fig. 4

$$p(Q) = \frac{\mathrm{j}\omega\rho_0}{2\pi}\int_{\mathrm{S}} \frac{\mathrm{e}^{-\mathrm{j}kr}}{r} v(P)\,\mathrm{dS} \tag{28}$$

where k is the wave number, ρ_0 is the air density, S is the area of the plate, r is the distance between the observation location Q and the centroid P of a triangular element.

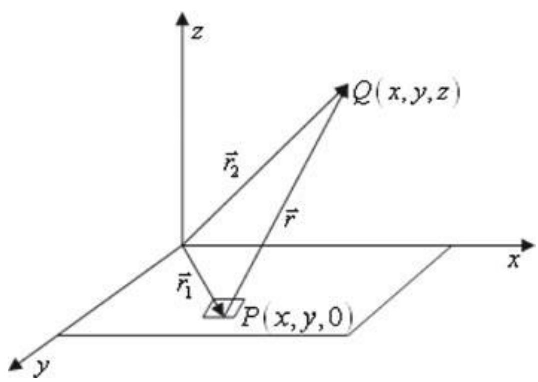

Figure 4. The sound pressure at an arbitrary observation location Q

The sound intensity at the observation location Q is defined as

$$I(Q) = \frac{1}{2}\mathrm{Re}\left[p(Q)v^*(Q)\right] \tag{29}$$

where $v^*(Q)$ is the complex conjugate velocity value at the observation location Q.

The sound power radiating into the semi-infinite space over the plate can be written as

$$W = \int_{S'} I(Q)\, \mathrm{d}S' \tag{30}$$

where S' is an arbitrary surface which cover the plate.

Substituting Eq. 28 and Eq. 29 into Eq. 30, and supposing S' is coincide with S, we can deduce[13]

$$W = \frac{\omega\rho_0}{4\pi} \int_{S'} \left[\int_{S} v(P) \frac{\sin(kr)}{r} v^*(Q)\, \mathrm{d}S \right] \mathrm{d}S' \tag{31}$$

where $v(P)$ is the normal velocity at location P, $v^*(Q)$ is the normal velocity at location Q.

By discretizing Eq. 31 into a finite form

$$W \approx \frac{\omega\rho_0}{4\pi} \sum_{i=1}^{N} \sum_{j=1}^{N} v(C_i) v^*(C_j) \frac{\sin kr}{r} (\Delta S)^2 = \mathbf{vZv}^* \tag{32}$$

where N is the total number of triangular elements, $v(C_i)$ is the normal centroid velocity of *i*th triangular element, and ΔS is the area of a triangular element.

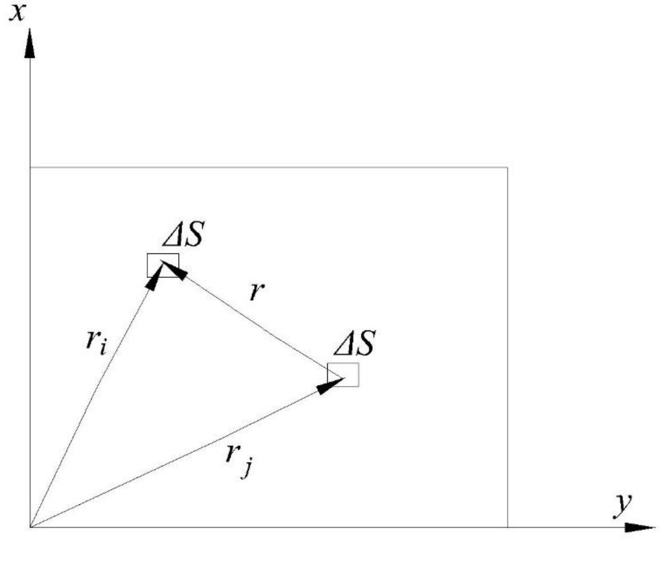

Figure 5. the discretization of a rectangular plate

$\mathbf{Z}$ is the sound resistance matrix defined as below[14]

$$\mathbf{Z} = \frac{\omega^2 \rho_0 S^2}{4\pi N c_0} \begin{bmatrix} 1 & \frac{\sin kr_{1,2}}{kr_{1,2}} & \cdots & \frac{\sin kr_{1,N}}{kr_{1,N}} \\ \frac{\sin kr_{2,1}}{kr_{2,1}} & 1 & \cdots & \frac{\sin kr_{2,N}}{kr_{2,N}} \\ \vdots & \vdots & \ddots & \vdots \\ \frac{\sin kr_{N,1}}{kr_{N,1}} & \frac{\sin kr_{N,2}}{kr_{N,2}} & \cdots & 1 \end{bmatrix} \tag{33}$$

where c_0 is the sound velocity in air.

Finally, the sound power level L_p of the plate can be defined as

$$L_p = 10 \log \frac{W}{W_0} \tag{34}$$

where W_0 is the reference sound power defined as 10^{-12} W.

5. Numerical example

Consider two rectangular plates that is simply supported and clamped. The length, width and thickness of the plates are 0.5 m, 0.4 m and 0.005m, respectively. The material parameters of the plates are given by Young's modulus 210 GPa; Poisson's ratio $v =$ 0.3 and the density $\rho =$ 7850 kg/m^3. A uniform discretization of 20 × 16 elements is used, as shown in Fig. 6.

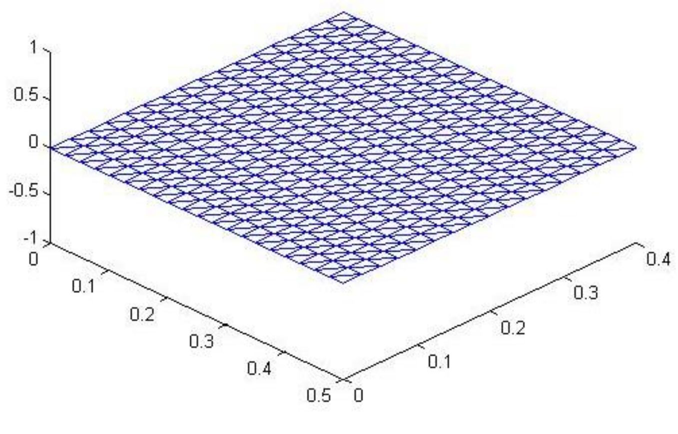

Figure 6. The mesh of a rectangular plate

For free vibration analysis, the eigen frequencies of the plates by the ES-FEM, together with the reference of the commercial software ANSYS are listed in Table 1 below. Fig. 7-9 is the mode shape of the clamped plate computed by ES-FEM and the ANSYS, Fig. 10-12 is the mode shape of the simply supported plate by ES-FEM and the ANSYS.

Table 1. The eigen frequencies results (Hz) of the plates from different methods

	The simply supported plate			The clamped plate		
Mode	ES-FEM (20 × 16)	ANSYS (20× 16)	ANSYS (high quality mesh)	ES-FEM (20 × 16)	ANSYS (20 × 16)	ANSYS (high quality mesh))
1	126.0	127.3	125.4	235.0	238.2	232.3
2	275.6	279.4	272.3	417.6	425.3	407.8
3	360.6	365.6	355.3	543.9	556.6	531.8
4	512.4	523.8	501.0	715.1	729.3	692.5
5	529.9	540.5	517.3	726.9	751.3	693.0

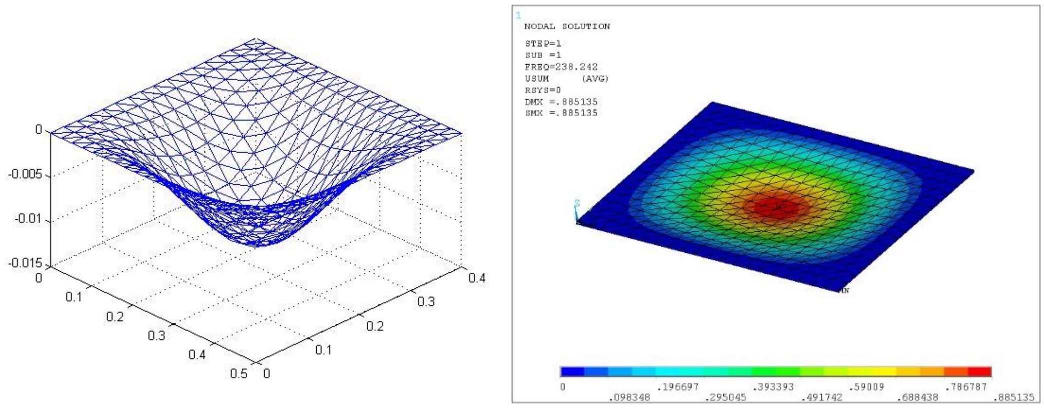

Figure 7. The first mode shape of the clamped plate

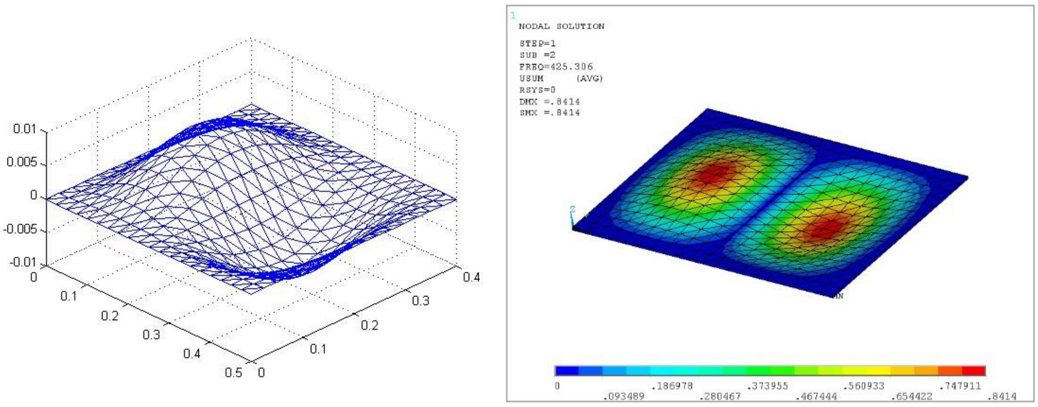

Figure 8. The second mode shape of the clamped plate

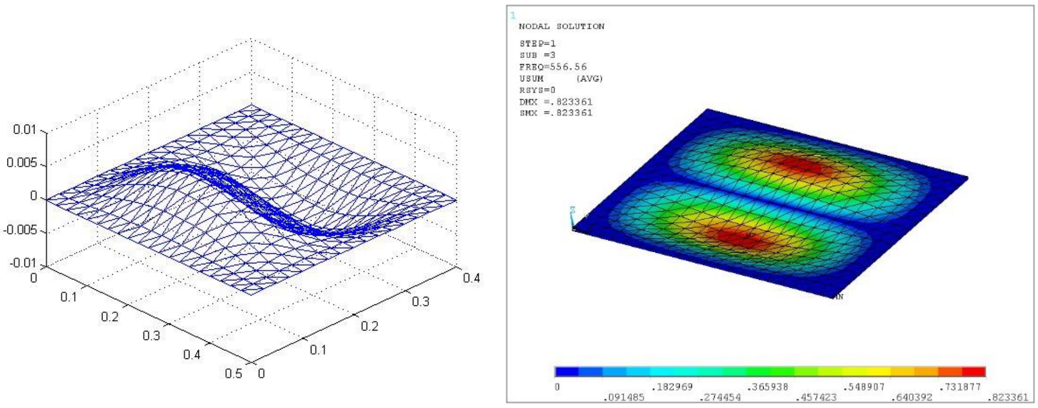

Figure 9. The third mode shape of the clamped plate

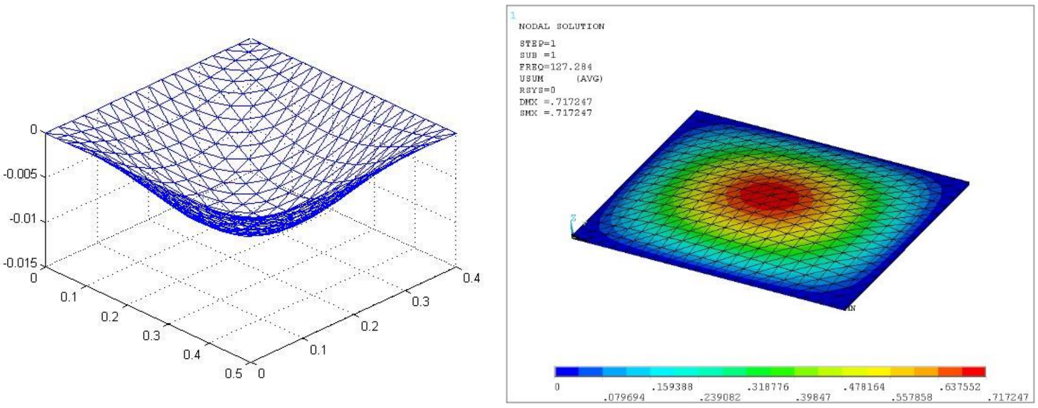

Figure 10. The first mode shape of the simply supported plate

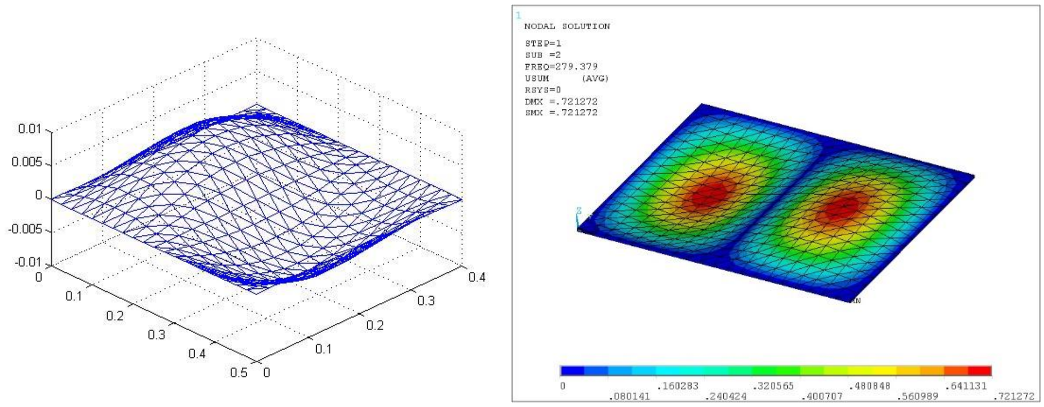

Figure 11. The second mode shape of the simply supported plate

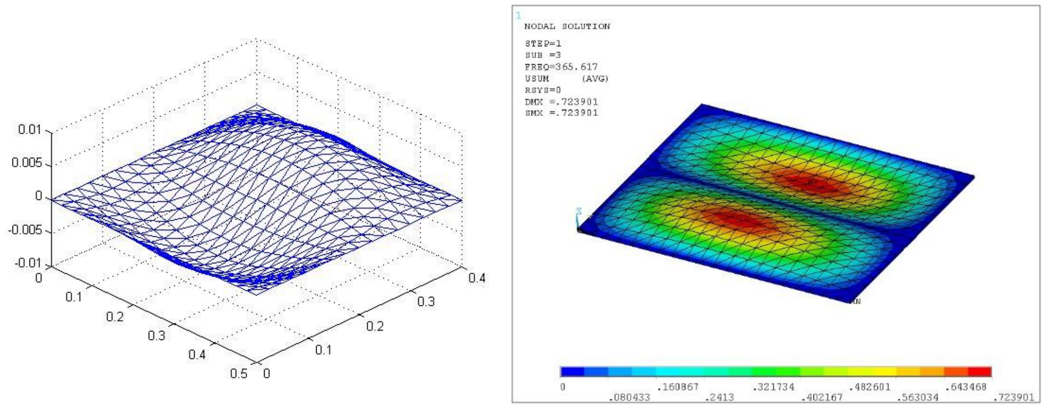

Figure 12. The third mode shape of the simply supported plate

From Table 1, it is observed that the results of the ES-FEM are more accurate than results of the commercial software ANSYS with the same mesh.

As shown in Fig. 13, the rectangular plate is subjected to a normal concentrated force 1 N on centroid of the surface. Then, computing sound power level of the plates from 1-1000 Hz in semi-infinite domain, together with the reference of the commercial software LMS Virtual.Lab are listed in Fig. 14-15. The density and velocity of air are defined as 1.205 kg/m^3 and 340 m/s.

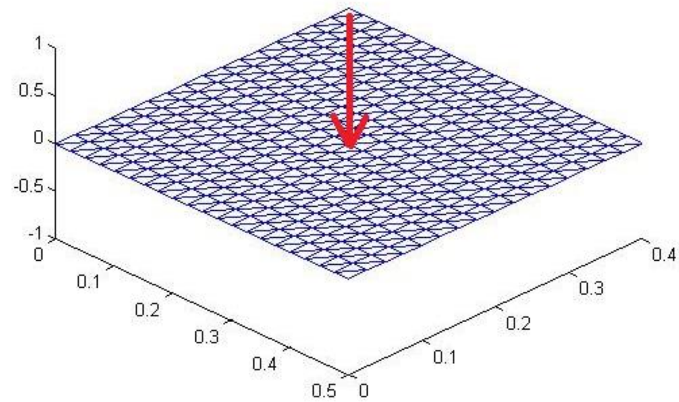

Figure 13. The rectangular plates with a concentrated force

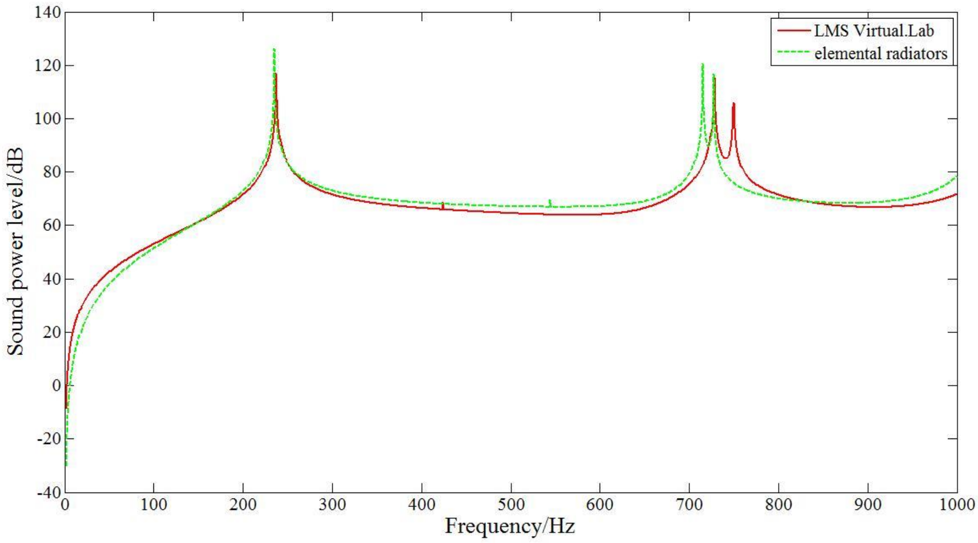

Figure 14. The sound power level of the clamped plates

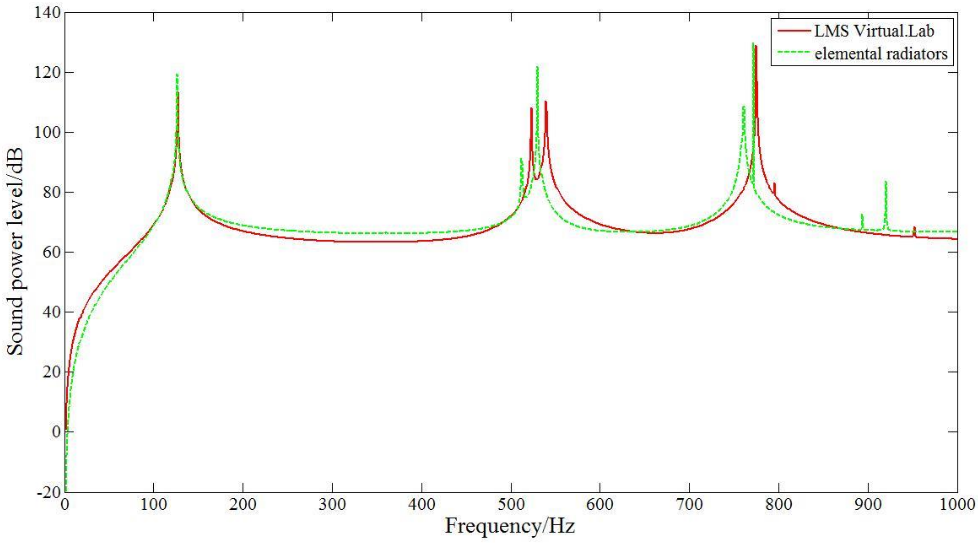

Figure 15. The sound power level of the simply supported plates

From Fig. 14-15, the results from elemental radiators are similar to the results from the Virtual.Lab, especially for the first peak. Due to the difference of two methods above in free vibration analysis, the rear peaks are slightly noncoincidence.

6. Conclusion

In this work, the edge-based smoothed finite element method with the Discrete Shear Gap is used in free vibration analysis of the plates, and the application of elemental radiators is utilized in sound radiation analysis. Through the numerical examples, some conclusion can be drawn below:

(1) The ES-DSG can give better accuracy than standard FEM in free vibration analysis using the same element mesh.

(2) The application of elemental radiators can not only provide a rapid computation, but manifest a desirable accuracy.

References

[1] M.Levinson (1985) Free vibrations of a simply supported rectangular plate, *Journal of Sound and Vibration* **98(2)**, 289–298.

[2] T. F. Raske, A. L. Schlack (1967) Dynamic response of plates due to moving loads, *Journal of the Acoustical Society of America* **42(3)**, 625-635.

[3] L. Fryba (1999) Vibration of solids and structures uder moving loads, Thomas Telford, London, UK.

[4] J. A. Gbadeyan, S. T. Oni. (1995) Dynamic behavior of beams and rectangular plates under moving loads, *Journal of Sound and Vibration* **182(5)**, 677–695.

[5] G. Maidanik (1974) Vibration and radiative classification of modes of a baffled finite panel, *Journal of Sound and Vibration* **34**, 447–455.

[6] C. E.Wallace (1972) Radiation resistance of rectangular panels, *Journal of the Acoustical Society of America* **53**, 946-952.

[7] E. G. Williams, J. D. Maynard (1982) Numerical evaluation of the Rayleigh integral for planar radiators using the FFT, *Journal of the Acoustical Society of America* **72(6)**, 2020-2030.

[8] K. U. Bletzinger, M. Bischoff, E. Ramm (2000) A unified approach for shear-locking free triangular and rectangular shell finite elements, *Comput. Struct* **75**, 321-334.

[9] Liu GR, Dai KY, Nguyen TT (2007) A smoothed finite element method for mechanics problems, *Comput Mech* **39**, 859–877.

[10] J. S. Chen, C. T. Wu, S. Yoon, Y. You (2001) A stabilized conforming nodal integration for Galerkin mesh-free methods, *International Journal for Numerical Methods in Engineering* **50**, 435-466

[11] Liu G. R., Nguyen-Thoi, T., and Lam, K. Y. (2009) An Edge-based Smoothed Finite Element Method (ES-FEM) for static, free and forced vibration analyses of solids, *Journal of Sound and Vibration* **320(4-5)**, 1100-1130.

[12] Rayleigh (1987) *The theory of sound*, 2nd edn, Dover Publications, New York, USA.

[13] Sung C. C., Jan, J. T. (1997) The response of and sound power radiated by a clamped rectangular plate, *Journal of sound and vibration* **207(3)**, 301-317.

[14] Qiao Y., Huang Q. (2007) Fluctuation strength of modulated sound radiated from rectangular plates with mixed boundary conditions, *Archive of Applied Mechanics* **77(10)**, 729-743.

[15] Zheng G., Cui X., Li G., Wu S. (2011) An edge-based smoothed triangle element for non-linear explicit dynamic analysis of shells, *Computational Mechanics*, **48(1)**, 65-80.